

## MIT Open Access Articles

*Fully Biodegradable Airway Stents Using Amino Alcohol-Based Poly(ester amide) Elastomers*

The MIT Faculty has made this article openly available. **Please share** how this access benefits you. Your story matters.

**Citation:** Wang, J., et al. "Fully Biodegradable Airway Stents Using Amino Alcohol-Based Poly(Ester Amide) Elastomers." *Advanced Healthcare Materials* 2 10 (2013): 1329-36.

**As Published:** 10.1002/ADHM.201200348

**Publisher:** Wiley

**Persistent URL:** <https://hdl.handle.net/1721.1/133918>

**Version:** Author's final manuscript: final author's manuscript post peer review, without publisher's formatting or copy editing

**Terms of use:** Creative Commons Attribution-Noncommercial-Share Alike



Published in final edited form as:

*Adv Healthc Mater.* 2013 October ; 2(10): 1329–1336. doi:10.1002/adhm.201200348.

## Fully Biodegradable Airway Stents Using Amino Alcohol-Based Poly(ester amide) Elastomers

Jane Wang<sup>[†]</sup>,

Charles Stark Draper Laboratory Biomedical Engineering Center Mail Stop 32, 555 Technology Square, Cambridge, MA 02139, USA; Massachusetts Institute of Technology 77 Massachusetts Ave, The David H. Koch Institute, Room 76-661, Cambridge, MA 02139-4307, USA

Kyle G. Boutin,

Charles Stark Draper Laboratory Biomedical Engineering Center Mail Stop 32, 555 Technology Square, Cambridge, MA 02139, USA

Omar Abdulhadi,

University of South Carolina 300 Main Street, Rm A219, Columbia, SC 2920

Lyndia D. Personnat,

Charles Stark Draper Laboratory Biomedical Engineering Center Mail Stop 32, 555 Technology Square, Cambridge, MA 02139, USA

Tarek Shazly [Prof.],

University of South Carolina 300 Main Street, Rm A219, Columbia, SC 2920

Robert Langer [Prof.],

Massachusetts Institute of Technology 77 Massachusetts Ave, The David H. Koch Institute, Room 76-661, Cambridge, MA 02139-4307, USA

Colleen L. Channick, M.D., and

Massachusetts General Hospital, 55 Fruit Street, Boston, MA, 02114, USA

Jeffrey T. Borenstein, Dr.\*

Charles Stark Draper Laboratory Biomedical Engineering Center Mail Stop 32, 555 Technology Square, Cambridge, MA 02139, USA

### Abstract

Airway stents are often used to maintain patency of the tracheal and bronchial passages in patients suffering from central airway obstruction caused by malignant tumors, scarring, and injury. Like most conventional medical implants, they are designed to perform their functions for a limited period of time, after which surgical removal is often required. Two primary types of airway stents are in general use, metal mesh devices and elastomeric tubes; both are constructed using permanent materials, and must be removed when no longer needed, leading to potential complications. This paper describes the development of process technologies for bioresorbable

prototype elastomeric airway stents that would dissolve completely after a predetermined period of time or by an enzymatic triggering mechanism. These airway stents are constructed from biodegradable elastomers with high mechanical strength, flexibility and optical transparency. This work combines microfabrication technology with bioresorbable polymers, with the ultimate goal of a fully biodegradable airway stent ultimately capable of improving patient safety and treatment outcomes.

## 1. Introduction

Most conventional medical implants are designed to perform a function for a specified period of time, and at the end of use, are either left behind in the implant site or surgically removed. With an expanded range of medical implants and increasing rates of use, renewed attention is being paid to inherent risks of sedation and infection from implant-retrieving surgeries as well as side effects arising from permanent implants. This has spurred interest in the development of fully biodegradable implants capable of reducing the costs associated with medical implants while enhancing patient safety.<sup>[1, 2]</sup> In response to this critical need, researchers have drawn on advances in scaffolding materials from the field of tissue engineering toward the development of a new generation of biodegradable implantable medical devices.<sup>[3, 4]</sup>

Airway stents are commonly used in patients with central airway obstruction secondary to malignant tumors, airway strictures, and tracheobronchomalacia<sup>[5–8]</sup> to maintain an open airway, thereby preventing morbidity and mortality due to hypoxia.<sup>[9]</sup> An ideal airway stent would preserve normal airway geometry and promote secretion clearance, minimize the formation of granulation tissue, not require removal following initial placement, and be made of inert material so as not to irritate the airway, precipitate infection, or promote granulation tissue.<sup>[10]</sup> It would also be available in multiple sizes and shapes for appropriate fitting to the patient, and possess sufficient mechanical strength to resist compressive forces while being sufficiently elastic to conform to airway contours. Two types of airway stents are currently available, silicone tube stents<sup>[11]</sup> and expandable metallic stents.<sup>[12]</sup> However, both types of existing stents are considered problematic with regard to their inability to maintain adherence to the airway and complications associated with device removal. They are also poorly suited for pediatric patients, due to the rapid growth rates of airway tissues in young patients.<sup>[9]</sup> While silicone stents help prevent the ingrowth of granulation tissue and are removable, they substantially alter airway mechanics and clearance, resulting in problems with retained secretions and airway obstruction.<sup>[13]</sup> In addition, silicone stents exhibit a relatively high risk of migration.<sup>[14]</sup> Expandable metal stents conform more closely to airway shape but are technically difficult to remove, in part due to tissue growth around the expandable metal structures.

In light of the abovementioned shortcomings, there exists an urgent need for the development of airway stents that maintain their position in the airway during treatment and do not require removal once they are no longer needed. Here we report on a prototype bioabsorbable airway stent device that is potentially capable of remaining in situ for a specified period of time, maintaining patency during the healing and remodeling process,

followed by a period of degradation to non-toxic byproducts.<sup>[15]</sup> This approach could also be useful for applications within the vasculature and esophagus as well as the airways, especially for pediatric patients who outgrow the stents at a rapid rate.<sup>[9]</sup>

A wide range of biodegradable polymers have been explored as scaffolding materials for tissue engineering and resorbable medical devices, including poly(lactic-glycolic acid) (PLGA),<sup>[16]</sup> poly(glycerol sebacate) (PGS),<sup>[17, 18]</sup> and silk fibroin.<sup>[19, 20]</sup> Early biodegradable implantable devices constructed using microfabrication technology with substrates such as PLGA and poly-caprolactone were demonstrated by Armani and Liu,<sup>[21]</sup> King et al.,<sup>[16]</sup> and Liu and Bhatia.<sup>[22]</sup> These structures suffered from excessive mechanical stiffness, spurring the development of devices comprised of biodegradable elastomers such as PGS, silk fibroin and polydioxanone (PDS)<sup>[23, 24]</sup> These studies have demonstrated the capability of microfabrication technology to produce biodegradable devices for implantation, but highlight the need for bioresorbable polymer substrate technologies with tunable degradation properties that would enable greater control over treatment strategies for these applications.

To develop a longer-lasting and tunably degradable substrate that preserves the excellent chemical and mechanical properties of PGS, a new class of biodegradable elastomers, poly(ester amide), poly(1,3-diamino-2-hydroxypropane-co-polyol sebacate) (APS), has been developed.<sup>[25]</sup> This family of APS polymers is highly tunable in both mechanical and degradation properties, and are composed of nontoxic, inexpensive monomers commonly used in biomedical devices and products. The relatively low Young's modulus, ranging between ~100 kPa to ~10 MPa,<sup>[26]</sup> and the tunable biodegradation half-life enable the material to exhibit biomimetic mechanical properties similar to those of extra-cellular matrix (ECM), and to achieve compatibility with dynamic mechanical environments. The hydrolysis rate and the elastic modulus of the polymer can both be tuned using different amide percentage and curing conditions. The polymer is also susceptible to enzymatic degradation, where the degradation rate of both the ester groups and amide groups can be individually and precisely triggered using different enzymes. By varying chemical composition as well as curing conditions over a wide range, degradation time can range between 6 weeks and one year, governed by multiple degradation mechanisms. The material has been shown to be highly biocompatible, with primary hepatocyte culture showing extended cell functionality without requiring deposition of protein coatings on the surface; it is also amenable to nanostructuring to provide topographical features representative of the cell microenvironment.<sup>[27]</sup>

## 2. Results and Discussion

### 2.1. Degradation of 2:1 APS and 1:2 APS

APS was synthesized via step-growth polymerization creating a network polymer consisted of ester and amide bonds, which is variable by manipulating the ratio of DAHP and glycerol in the starting materials. Esterases and aminopeptidases were considered good candidates for the triggered degradation of APS, as they target the ester and amide bonds respectively. Protease, lipase, and DPBS (control) were incubated with APS over 8 weeks of time to identify the most effective enzyme for triggering the degradation of APS. The comparison of

degradation rates between 2:1 (diamine:glycerol) APS and 1:2 APS showed that lipase effectively degraded APS, and showed selectivity in acceleration of degradation toward 1:2 APS up to 40% in 8 weeks (Figure 1). There were no significant differences between the degradation rate of 2:1 APS in protease, lipase, and the control over 8 weeks (Figure 1a), while prominent degradation in 1:2 APS with lipase was observed (Figure 1b). 1:2 APS degraded about 8% via hydrolysis in DPBS over 8 weeks, but up to 40% by lipase solution. It was determined that by varying the ratio of diamine to glycerol (2:1 for 2:1 APS and 1:2 for 1:2 APS), the degradation rate of APS in lipase was highly tunable. The lower the diamine content, the faster the polymer responded to lipase solution as a catalyst for degradation.

Scanning Electron Microscope images of the cross-section of degraded 1:2 APS samples using Hitachi S3500N Scanning Electron Microscope were taken (Figure 2). From Figure 2a, surface roughening of 1:2 APS was observed within mere 4 days of degradation. Over 8 weeks of time, 1:2 APS decreased steadily in thickness while maintaining structural integrity (Figure 2b). Therefore, the degradation mechanism of APS was identified as surface erosion (Figure 2c), which may be particularly useful for medical devices that require consistent device mechanical integrities and functionalities before complete degradation. The effect of lipase concentration on the rate of degradation of 1:2 APS was also explored (Figure 3). By increasing the concentration of enzyme solution by 10-fold, the degradation rate of 1:2 APS increased by about 50%.

These results indicated that the degradation rate of APS may be controlled over a wide range of diamine to glycerol ratios, as well as by the particular enzyme selected and the concentration of the enzyme. Lipase solution at designated concentrations may be used to trigger degradation of airway stents constructed from 1:2 APS. A possible approach toward delivery of the enzymatic trigger is to flow the enzyme solution through the airway; since APS goes through surface erosion, it is not necessary to fully immerse the stents in solution in order to achieve enzymatic degradation. The enzyme can be administered via nebulizers and inhalers.

## 2.2. Mechanical Properties of APS compared to PDMS

Mechanical properties of 24 hour cured 1:2 APS, 48 hour cured 1:2 APS, 2:1 APS, and PDMS as a reference material for silicone stents have been measured and are summarized in Figure 4 below. The Young's Moduli for these materials were measured to be  $2.32 \pm 0.11$  MPa,  $6.28 \pm 0.30$  MPa,  $2.21 \pm 0.17$  MPa, and  $2.40 \pm 0.14$  MPa respectively. As the stiffness values of 48 hour cured 1:2 APS scaffolds were nearly three times higher than those of 24 hour cured scaffolds, we concluded that a 24 hour cure was the optimal scaffold preparation time in order to achieve desired mechanical properties, which were assumed to be close to those observed in silicone stents. The 24 hour cured 1:2 APS and 24 hour cured 2:1 APS exhibited mechanical properties very similar to PDMS, indicating the airway stents made with 24 hour cured APS, regardless of the composition of diamine and glycerol, were comparable in mechanical integrity to that of existing stents made with silicone. Other common biodegradable polymers used for airway stents, such as Poly-L-Lactic Acid (PLLA) with a Young's modulus in the range of 6.9–9.8 GPa<sup>[28]</sup> would likely have

excessive stiffness for this application. Poly(Glycerol Sebacate) (PGS), with a Young's Modulus in the range of 200–800 kPa,<sup>[29]</sup> would likely be too soft, suggesting APS as the closest biodegradable polymer in mechanical properties to PDMS.

As the Young's modulus of APS and PDMS both fell in the range of 2 MPa, the comparable mechanical properties suggested that APS is a viable material to replace common silicone stents. Prototypes made using 1:2 APS were both strong and elastic.

### 2.3. Nanopatterning APS and Adhesive Mechanical Test against Porcine Trachea Tissue

Earlier literature reports have pointed toward the use of nanostructured surfaces to achieve high adhesive forces without the use of large, unwieldy structures such as the posts on the surface of silicone stents. In the work of Mahdavi et al., nanopatterned surfaces exhibited strong vertical adhesion to surfaces.<sup>[30]</sup> We proposed using surface nanopatterns to enhance the adhesion of airway stents to tissue to reduce the risk of migration and to avoid the need for the large posts that cause tissue trauma during placement and removal of silicone stents. In order to test the influence of selected nanopatterns imprinted in APS films, (Figure 5), nanopatterned APS scaffolds with nanogratings in size of 500, 750, and 1000 nm, were created via print molding, and tested mechanically against porcine trachea tissue. The SEM images in Figure 5b and 5d of the cross-section of print molded APS indicated that though the feature is created after the thin film had already been cured, the nano-featured layer had fully crosslinked with the surface of thin film.

The adhesive interaction of nanopatterned materials with tracheal tissue samples approximately 1 cm<sup>2</sup> in surface area excised from pigs was assessed through the load response to a parallel interfacial displacement. All nanopatterned materials exhibited greater interfacial displacements as compared to flat, unpatterned samples. The strength of the effect of the nano-pattern increased with the size of the nanostructure imprinted on the APS surface, with the 1000 nm variant exhibiting the highest load response over the examined range (Figure 6a). The interfacial stiffness was characterized by the linearized load response over small displacements (0–0.1 mm), and is significantly enhanced through surface nanopatterning (Figure 6b).

This initial study of surface adhesion of nanopatterned APS films to excised tracheal tissue samples was done using flat samples tested in a planar configuration. A more realistic test of the use of nanopatterning to achieve elevated adhesive forces between the stent and tracheal surface would utilize cylindrical airway prototypes inserted into intact tracheal tubes. This is a far more complex test that is planned for future studies, but the most significant initial challenge is the requirement for transferring a nanopattern onto the outer surface of the cylindrical airway stent.

### 2.4. Synthesizing Prototype Airway Stents from 1:2APS

The dehydration process of APS prepolymer plays a vital role in the formation of crosslinkages, and is traditionally achieved by reverse molding on silicon wafers.<sup>[26]</sup> APS prepolymer was melted on wafers and water molecules were removed through the upper face of polymer under vacuum. Cured APS thin films were then delaminated and rolled into

cylinders with a side seal using APS prepolymer as glue. This method enabled the creation of cylindrical shape tubes.

As mentioned in section 2.3, nanopatterned APS scaffolds showed superior capabilities in displacement resistance. It is thus important to built airway stents with nanopattern on the outside surface, to capture both the concepts of bioresorbable and displacement resisting. Upon implantation, the nanogratings will help with the adhesion of stents toward the airway, while endothelization and cell proliferation also begins for wound healing on the adhesion site. Nanopatterning on polymeric materials are traditionally done by reverse molding of silicon wafers<sup>[31]</sup> and electrospinning.<sup>[32]</sup> Electrospinning was considered less applicable due to the low consistency between nanofibers, making it difficult to create precise and repeating nanopattern. Nanopatterned APS thin films were instead created via reverse molding from nanograted silicon wafers. These nanopatterned films could then be rolled into a cylindrical tube, with the nanopattern facing the outside surface of the cylinder in order to contact and grip the trachea. However, when investigating the mechanical integrity of the rolled up prototypes, it was observed that these prototypes suffer from high rate of failure around the seal area due to stress and buckling, as shown in Figure 7a. Presumably, stress around the seal would push the cylinder stent into a droplet shape, and eventually crack along the seam, thereby causing the stent to lose its function in maintaining an open airway.

This setback required exploration of new approaches toward fashioning a cylindrical tube stent. In order to build more robust airway stents using APS, casting from metal and Teflon stent molds in cylindrical shapes was considered. However, poor solvent transport through the bulk mold became a major problem, impeding the removal of water from the prepolymer for crosslinkage formation. As an alternative, porous Teflon molds with cylindrical shapes were used for crosslinking of APS prepolymer into a hollow cylinder with the appropriate radius, length and wall thickness. The porous nature of the mold structure enabled solvent absorption during the curing process, so that all solvent was not forced to the outside surface of the APS film during curing. We found that proper selection of pore size was critical in balancing the tradeoff between insufficient transport (for low porosity molds) and leakage of APS molecules through the mold (for molds with large pores) (Figure 7b-c). In addition, the surface properties of the mold, including the porosity and pore size, were found to be critical in ensuring stent delamination from mold without need for a sacrificial layer. As seen in Figure 7d-e, different sizes of airway stents were molded into device sizes suitable for fitting in tracheal tubes and bronchial tubes, respectively. Porous Teflon molds were also manually patterned using biopsy punches to mimic existing airway stents with studs (Figure 7f).

Initial approaches toward fabricating nanopatterned airway stents, done via rolling up nanopatterned thin film, resulted in significant deformations and deviations from a true cylinder, and spurred the transition to a de-molding process utilizing a cylindrical mold, as described above. This new method of stent molding highlighted the need for an alternative to the traditional reverse molding method, as the replication of surface patterning on a flat surface requires subsequent rolling into a cylinder. Since it is very difficult to create a nanopattern on the cylindrical porous Teflon mold, an alternative nanopatterning method was introduced: the print molding method, which had been proven effective in the creation of nanopatterns on APS as in Figure 5. Since PDMS is a flexible polymer easily nano-



patterned from reverse molding, nanopatterned PDMS thin films can be spun with maltose coating and adhered to stents that were delaminated from porous Teflon molds with small amount of APS melted on top. The flexibility of PDMS should enable the nanopatterning of readily made stents without deforming them. The actual application of print molding on cylindrical stent will be the next step of stent creation process for the full trachea displacement tests.

### 3. Conclusion

To our knowledge this is the first report of a biodegradable elastomeric airway stent composed of the alcohol-based poly(ester amide) elastomer, APS. This material possesses a slower degradation rate compared to polymeric material currently used in tissue engineering,<sup>[29, 33]</sup> while retaining elastomeric properties for implant flexibility in airways. Utilizing the process described here, we were able to create molded airway stents that varied in length, diameter, wall thickness, degradation rate, and size of nano-grating on the surface. By varying the amine to glycerol ratio and concentration of enzyme, the degradation properties of APS can be tuned, the capability to trigger the degradation at designated time via the introduction of enzyme to the stents enabled precise control over the degradation of devices. Since the mechanical properties of these APS scaffolds with various compositions were similar to that of PDMS, the degradation rate of stents was highly tunable without the risk of losing mechanical strength.

Print molding, a new topographic processing method, was developed to allow for surface patterning of the stents. Use of the print molding technique enabled nanopatterning of scaffolds to be freed from the limitation of patterning on flat silicon surfaces. With the nanopatterned APS showing significant displacement resistance, nanopatterning APS airway stents emerges as a viable approach toward avoidance of dislodging of stents without the use of large posts that can cause tissue injury upon placement. Mechanical testing showed that 1000 nm nanogratings on APS enhanced the resistance to interfacial displacement against porcine trachea tissue compared to that of flat surfaces. The biocompatibility of APS *in vivo* by Bettinger et al.<sup>[34]</sup> demonstrated that the material and its by products are biocompatible and resorbable, and was suitable for resorbable tissue engineering devices for the purpose of drug delivery and regenerative medicine. Future directions for this technology may comprise seeding of respiratory tract endothelial cells to explore regenerative application of these biodegradable airway stents, *in vivo* biocompatibility, host integration and long-term degradation properties.

### 4. Experimental Section

#### APS Synthesis

1) Poly(1,3-diamino-2-hydroxypropane-co-polyol sebacate)s Prepolymer: All materials were purchased from Sigma Aldrich (St. Louis, MO, USA) and used as received unless otherwise specified. The polymer formulation 2DAH-1G (2:1 APS) was synthesized as described in Bettinger et. al,<sup>[25]</sup> and 1DAH-2G (1:2APS) was synthesized in similar manners with the following changes. A round bottom flask was charged with 1,3-diamino-2-hydroxy-propane (DAH) (0.166 mol), glycerol (G) (0.332 mol), and sebacic acid (SA) (0.499 mol) to



produce a molar ratio of 1:2:3 of DAP:G:SA, respectively. The reactants were heated under an argon blanket at 130 °C for 2 h. The pressure was then dropped to approximately 50 mTorr and the contents were allowed to react for 8 h at 130 °C. The product was then stored under a desiccant environment until further use.

2) APS Thin Films: Single side polished silicon wafers were oxygen plasma-cleaned (March, St. Petersburg, FL) at 250 mTorr and 200 W for 45 seconds. A 60% (w/w) solution of maltose (Sigma, St. Louis, MO) in water was spin-coated at 2500 revolutions per minute for 30 s. The maltose layer was pre-baked on a hot plate at 95 °C for 120 seconds. Film thickness of 0.5 mm was achieved by spreading the prepolymer at surface densities of 100 mg/cm<sup>2</sup> at 170 °C for smooth sheet formation. The prepolymer was cured at 170 °C for 24 hours under 50 mTorr of vacuum, which produced a crosslinked sheet. The APS sheets were delaminated by statically incubating the polymer-wafer system in doubly distilled water (ddH<sub>2</sub>O) at 70 °C for 18 h beginning immediately after polymer curing. Diffusion of water between the polymer/silicon interfaces led to maltose dissolution and eventual delamination. Sol was removed by incubating polymer films in 100% ethanol for 24 hours followed by washing and incubation with ddH<sub>2</sub>O.

### Degradation of APS

1) APS Degradation Over 8 Weeks: 2:1 APS and 1:2 APS thin films were punched using biopsy punches (7 mm diameter) to create cylindrical polymer slabs (n = 3) with dimensions of 0.5 mm × 7 mm (T × D) and weighing each (~20 mg) were incubated at 37 °C in the following degradation media: (1) Dulbecco's Phosphate Buffer Saline (DPBS); (2) protease I from bovine pancreas (10 U mL<sup>-1</sup>) in DPBS; (3) lipase II from porcine pancreas (10 U mL<sup>-1</sup>) in DPBS. Buffer and enzyme solutions were exchanged every 2 days and dry mass loss measurements were made every week of fresh samples. Samples were washed in ddH<sub>2</sub>O, incubated in ethanol and ddH<sub>2</sub>O for at least 24 h. Dry mass were weighed for mass loss comparison.

2) The Effect of Concentration of Enzyme to Degradation Rate: 2:1 APS and 1:2 APS thin films were punched using biopsy punches (7 mm diameter) to create cylindrical polymer slabs (n = 3) with dimensions of 0.5 mm × 7 mm (T × D) and weighing each (~20 mg) were incubated at 37 °C in the following degradation media: (1) lipase II from porcine pancreas (10 U mL<sup>-1</sup>) in DPBS; (2) lipase II from porcine pancreas (20 U mL<sup>-1</sup>) in DPBS; (3) lipase II from porcine pancreas (40 U mL<sup>-1</sup>) in DPBS; (4) lipase II from porcine pancreas (100 U mL<sup>-1</sup>) in DPBS. Buffer and enzyme solutions were exchanged everyday and dry mass loss measurements were made every week of fresh samples. Samples were washed in ddH<sub>2</sub>O, incubated in ethanol and ddH<sub>2</sub>O for at least 24 h. Dry mass were weighed for mass loss comparison.

### Airway Stent Molding

Porous Teflon tubes (ID 3/8", OD 5/8") and flat sheets (0.25" thick) with 0.8 µm pore size were purchased from FluoroTechniques Membrane Products, Inc. (Castleton, NY, USA) and used as received unless otherwise specified. Teflon rods (5/16") were purchased from VWR (Radnor, PA, USA). 5 cm long Teflon rods were mounted on the center of 1.5 cm by 1.5 cm

square porous Teflon sheets, and Dow Corning 1044 Silicone Rubber RTV coating (Dow Corning, Midland, MI) was used to seal sheet-tubing interfaces. 5.25 cm long porous Teflon tubes were mounted over the centered Teflon rods and sealed. Melted APS prepolymer was poured into the mold slowly and set to cool at room temperature for 4 hours, and sealed with another 1.5 cm by 1.5cm square porous Teflon sheets. The filled molds are cured at 170 °C at approximately 50 mTorr for 24 hours, and removed from the mold using razor blades.

### Mechanical Testing

The thicknesses of APS films were determined by measuring at the five separate points across the sample with a dial gauge (L.S. Starrett, Athol, MA). The samples were cut using a dog bone shape specimen cutter to size  $2.0 \times 5.0 \text{ mm}^2$ , and mounted on an Electroforce ELF 3200 mechanical tester (Bose-Enduratec, Framingham, MA) with a 500N load cell (model 31-1435-03; Sensotech, Columbus, OH). The samples were elongated to failure.

### Nanot-Patterning by Print Molding

Polystyrene nanopatterned mold was generated from hot embossing of a nickel mold created by Frohlich et al.<sup>[35]</sup> Thin PDMS mold was reverse molded from mixing PDMS elastomer and curing agent (Sylgard 184, Dow Corning, Midland, MI) in a 10:1 ratio by weight, poured onto the nano-patterned polystyrene mold, degassed in vacuum for 30 min, and cured in a 65 °C oven for 3 hours to create thin films of thickness  $0.50 \pm 0.05 \text{ mm}$ . Thin films were then oxygen plasma-cleaned (March, St. Petersburg, FL) at 250 mTorr and 200 W for 45 seconds, and spun with a 90% (w/w) solution of maltose (Sigma, St. Louis, MO) in water at 2500 revolutions per minute for 30 s. The maltose layer was pre-baked on a hot plate at 95 °C for 120 seconds. 0.5 g of APS prepolymer is then melted on the nanopatterned, and then adhered to a flat, fully cured APS thin film as described above. The polymer combination was cured at 170 °C for 24 hours under 50 mTorr of vacuum with weight on top. The APS sheets were delaminated by statically incubating the polymer-master system in doubly distilled water (ddH<sub>2</sub>O) at 60 °C for 24 hours beginning immediately after polymer curing. Diffusion of water between the polymer/silicon interfaces led to maltose dissolution and eventual delamination.

### Adhesive Mechanical Test of Nano-Patterned APS against Porcine Trachea Tissue

A modified shear test was used to rate the adhesion force between excised samples of porcine tracheal tissue ( $100 \text{ mm}^2$ ) and three variants of nanopatterned materials (500, 750, and 1000 nm). Rectangular material ( $10 \times 15 \text{ mm}^2$ ) and tissue samples were secured within the upper and lower arms of a mechanical testing system (Bose Enduratec) configured for uniaxial displacement, such that the interface between the two was parallel to the direction of imparted motion. Prior to mechanical testing, a constant setting force of 1N was applied in the normal direction to the tissue-material construct for 1 minute, providing repeatable conditions for initiation of mechanical testing. Uniaxial displacement was applied to the tissue-material constructs at a rate of 0.05 mm/sec in the direction parallel to interface, and system software (Wintest) was used to continuously record the resultant load (50 data points/sec). A constant contact area ( $10 \text{ mm}^2$ ) was retained between the tissue and material samples throughout the test.

## Acknowledgments

Funding for this work, provided by Draper Laboratory and by the Center of Integration of Medicine and Innovative Technology, Contract Number US Army DAMD17-02-2-0006, is gratefully acknowledged. We are indebted to G.C. Engelmayr, C.J. Bettinger, L.E. Freed, J. Hsiao, M.E. Kolewe and H.S. Park for many useful discussions and assistance with the instrumentation and polymer synthesis.

## References

- [1]. Langer R, Vacanti JP. *Science*. 1993; 260:920–6. [PubMed: 8493529]
- [2]. Griffith LG, Naughton G. *Science*. 2002; 295:1009–1014. [PubMed: 11834815]
- [3]. Hofmann GO. *Arch. Orthop. Trauma Surg.* 1995; 114:123–132. [PubMed: 7619632]
- [4]. Gupta B, Revagade N, Hilborn J. *Prog. Polym. Sci.* 2007; 32:455–482.
- [5]. Carden KA, Boisselle PM, Waltz DA, Ernst A. *Chest*. 2005; 127:984–1005. [PubMed: 15764786]
- [6]. Cooper JD, Pearson FG, Patterson GA, Todd TR, Ginsberg RJ, Goldberg M, Waters P. *Ann. Thorac. Surg.* 1989; 47:371–8. [PubMed: 2467629]
- [7]. Lemaire A, Burfeind WR, Toloza E, Balderson S, Petersen RP, Harpole DH Jr. D'Amico TA. *Ann. Thorac. Surg.* 2005; 80:434–7. [PubMed: 16039180]
- [8]. Wood DE, Liu YH, Vallieres E, Karmy-Jones R, Mulligan MS. *Ann. Thorac. Surg.* 2003; 76:167–72. [PubMed: 12842534]
- [9]. Ernst A, Feller-Kopman D, Becker HD, Mehta AC. *Am. J. Respir. Crit. Care Med.* 2004; 169:1278–97. [PubMed: 15187010]
- [10]. Ernst A. *Am. J. Resp. Crit. Care Med.* 2004; 169:1081–1082. [PubMed: 15132955]
- [11]. Liu Y-H, Ko P-J, Wu Y-C, Liu H-P, Tsai Y-H. *Asian Cardiovasc. Thorac Ann.* 2005; 13:178–180. [PubMed: 15905351]
- [12]. Colt HG, Dumon JF. *Clin. Chest Med.* 1995; 16:465–78. [PubMed: 8521701]
- [13]. Dumon J-F, Cavaliere S, Diaz-Jimenez JP, Vergnon J-M, Venuta F, Dumon M-C, Kovitz KL. *J. Bronchol.* 1996; 3:6–10.
- [14]. Dumon JF. *Chest*. 1990; 97:328–32. [PubMed: 1688757]
- [15]. Thornton RH, Gordon RL, Kerlan RK, LaBerge JM, Wilson MW, Wolanske KA, Gotway MB, Hastings GS, Golden JA. *Radiology*. 2006; 240:273–82. [PubMed: 16793984]
- [16]. King KR, Wang CCJ, Kaazempur-Mofrad MR, Vacanti JP, Borenstein JT. *Adv. Mater.* 2004; 16:2007.
- [17]. Fidkowski C, Kaazempur-Mofrad MR, Borenstein J, Vacanti JP, Langer R, Wang YD. *Tissue Eng.* 2005; 11:302–309. [PubMed: 15738683]
- [18]. Bettinger CJ, Weinberg EJ, Kulig KM, Vacanti JP, Wang YD, Borenstein JT, Langer R. *Adv. Mater.* 2006; 18:165. [PubMed: 19759845]
- [19]. Bettinger CJ, Cyr KM, Matsumoto A, Langer R, Borenstein JT, Kaplan DL. *Adv. Mater.* 2007; 19:2847. [PubMed: 19424448]
- [20]. Borenstein JT, Tupper MM, Mack PJ, Weinberg EJ, Khalil AS, Hsiao J, Garcia-Cardena G. *Biomed. Microdevices*. 2010; 12:71–79. [PubMed: 19787455]
- [21]. Armani DK, Liu C. *J. Micromech. Microeng.* 2000; 10:80–84.
- [22]. Liu Tsang V, Chen AA, Cho LM, Jadin KD, Sah RL, DeLong S, West JL, Bhatia SN. *FASEB J.* 2007; 21:790–801. [PubMed: 17197384]
- [23]. Vondrys D, Elliott MJ, McLaren CA, Noctor C, Roebuck DJ. *Ann Thorac Surg.* 92:1870–4. [PubMed: 22051281]
- [24]. Lischke R, Pozniak J, Vondrys D, Elliott MJ. *Eur. J. Cardiothorac. Surg.* 2011; 40:619–24. [PubMed: 21334911]
- [25]. Bettinger CJ, Bruggeman JP, Borenstein JT, Langer RS. *Biomaterials*. 2008; 29:2315–2325. [PubMed: 18295329]
- [26]. Wang J, Bettinger CJ, Langer RS, Borenstein JT. *Organogenesis*. 2010; 6:212–6. [PubMed: 21220957]

- [27]. Bettinger CJ. Pure App. Chem. 2009; 81:2183–2201.
- [28]. Fukushima K, Kimura Y. Polym. Int. 2006; 55:626–642.
- [29]. Wang YD, Ameer GA, Sheppard BJ, Langer R. Nat. Biotechnol. 2002; 20:602–606. [PubMed: 12042865]
- [30]. Mahdavi A, Ferreira L, Sundback C, Nichol JW, Chan EP, Carter DJ, Bettinger CJ, Patanavanich S, Chignozha L, Ben-Joseph E, Galakatos A, Pryor H, Pomerantseva I, Masiakos PT, Faquin W, Zumbuehl A, Hong S, Borenstein J, Vacanti J, Langer R, Karp JM. Proc. Nat. Acad. Sci. USA. 2008; 105:2307–12. [PubMed: 18287082]
- [31]. Bettinger CJ, Kulig KM, Vacanti JP, Langer R, Borenstein JT. Tissue Eng. Part A. 2009; 15:1321–9. [PubMed: 18847357]
- [32]. Barnes CP, Sell SA, Boland ED, Simpson DG, Bowlin GL. Adv Drug Deliv. Rev. 2007; 59:1413–33. [PubMed: 17916396]
- [33]. Agrawal CM, Ray RB. J. Biomed. Mater. Res. 2001; 55:141–50. [PubMed: 11255165]
- [34]. Bettinger CJ, Kulig KM, Vacanti JP, Langer R, Borenstein JT. Tissue Eng. Part A. 2009; 15:1321–1329. [PubMed: 18847357]
- [35]. Frohlich EM, Zhang X, Charest JL. Integ. Biol. 2012; 4:75–83.

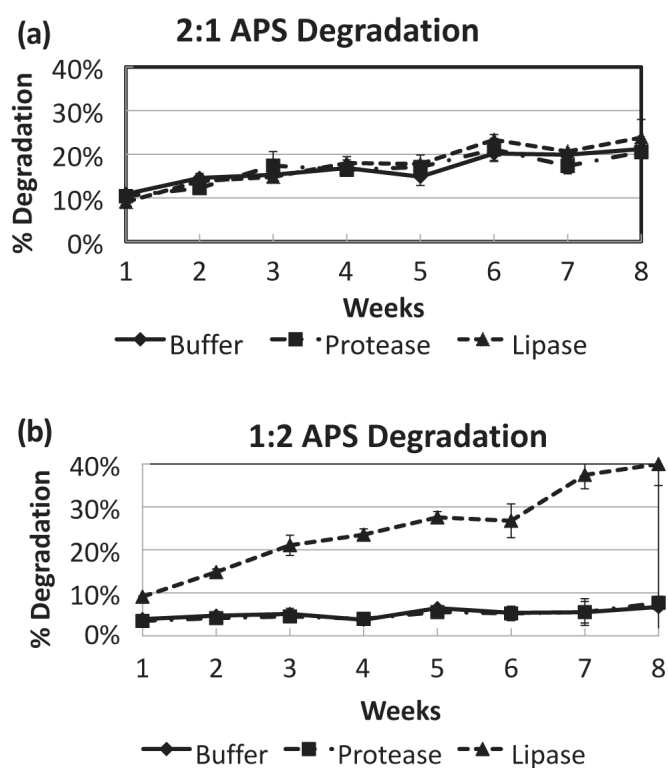


**Figure 1.**

1:2 and 2:1 APS degradation over 8 weeks in buffer, protease, and lipase solution. a) 2:1 APS showed consistent degradation rates regardless the presence of enzyme. b) 1:2 APS showed selective degradation up to 40% in 8 weeks at the presence of lipase solution.

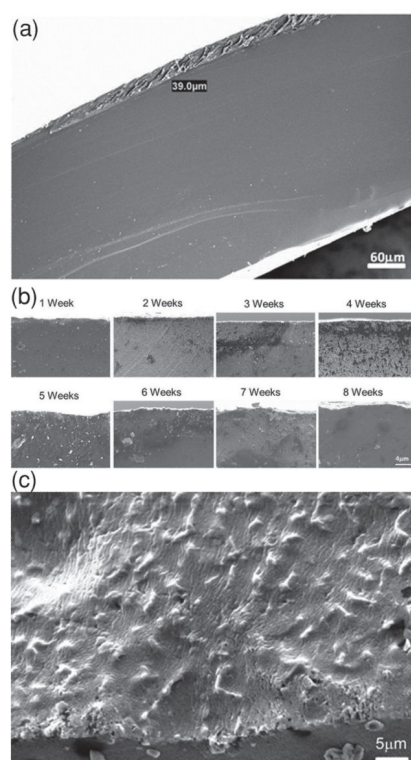


**Figure 2.**

SEM images of 1:2 APS degradation under lipase. a) Within 4 days of degradation in lipase solution, 39 μm of surface erosion was observed. b) Degradation of 1:2 APS continued over 8 weeks at the presence of lipase solution. c) Surface erosion of 1:2 APS by lipase solution at week 5.

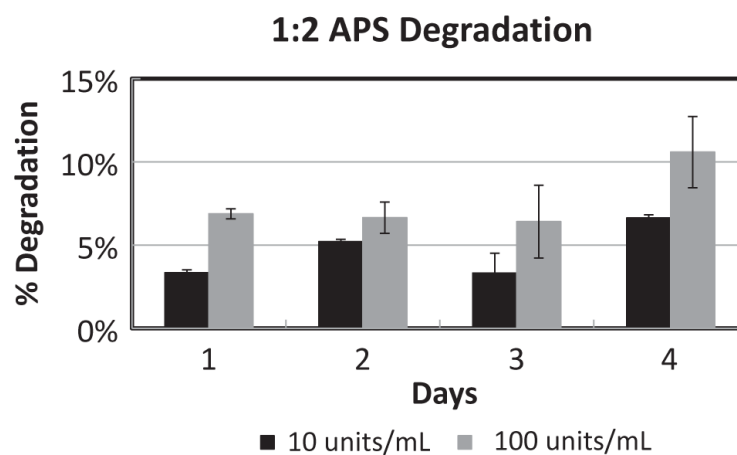


**Figure 3.**  
Change in degradation rate of 1:2 APS by varying lipase concentration.



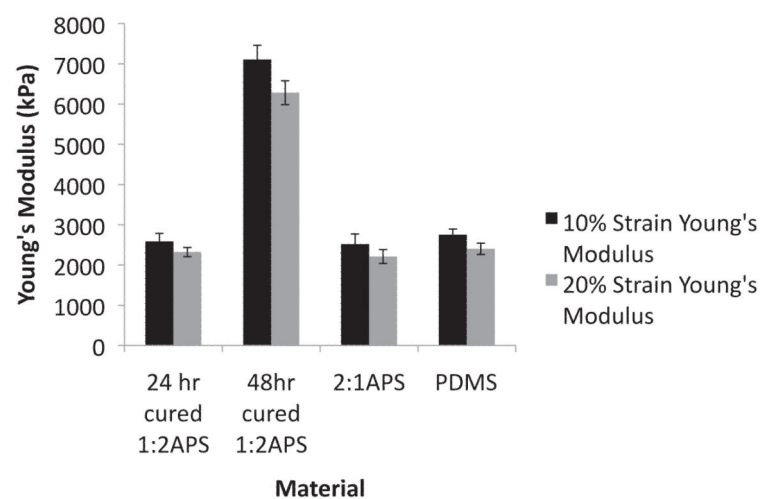


**Figure 4.** Young's modulus of 24 hour cured 1:2 APS, 48 hour cured 1:2 APS, 24 hour cured 2:1 APS, and PDMS each at 10% strain and 20% strain.

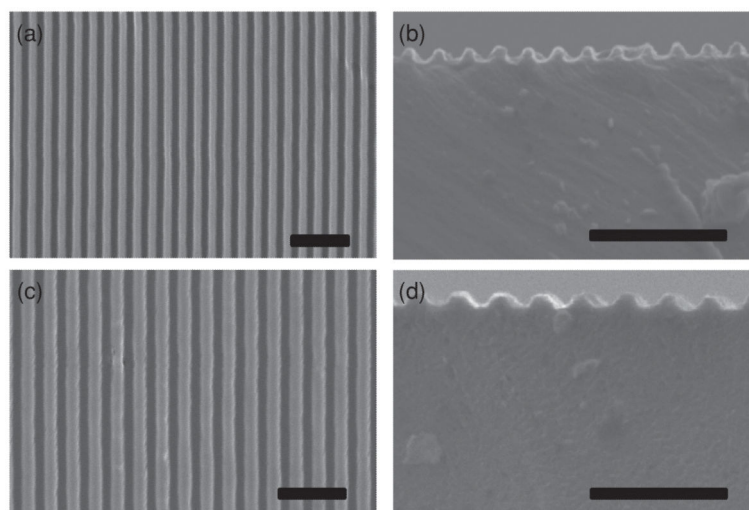


**Figure 5.** SEM images of 1:2 APS scaffolds with nano-gratings in sizes a) 500 nm from top view, b) 500 nm from cross section view, c) 750 nm from top view, and d) 750 nm from cross section view. (Scale bars represent 5  $\mu\text{m}$ .)

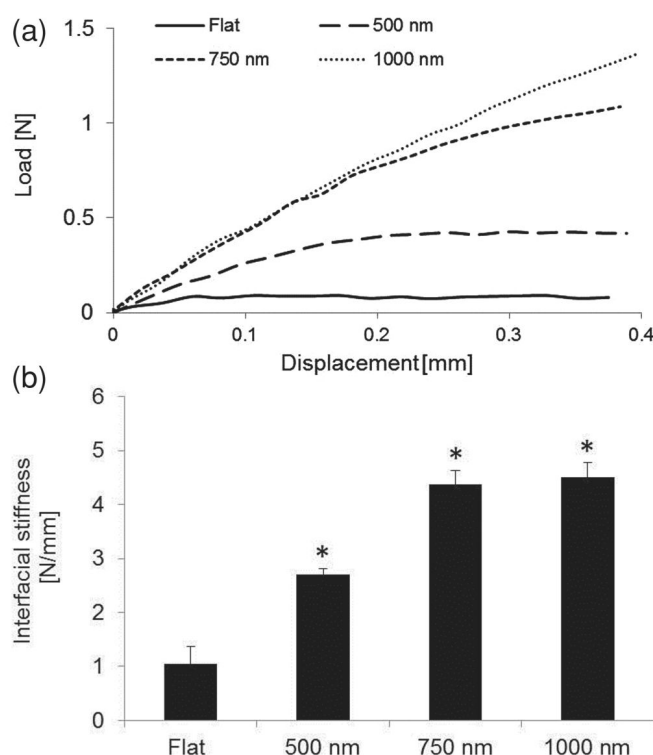


**Figure 6.**

A modified shear test was used to rate the interfacial adhesion strength of tissue-material constructs. (a) A representative plot of the load-response of tissue-material constructs formed with either flat or nanopatterned materials. (b) The interfacial stiffness of tissue-material constructs was calculated based on a linearization of the load response over small displacements, and is significantly increased by nanopatterning. Error bars represent 1 standard deviation ( $n = 4$ ) and \* denotes a statistical difference from the flat material ( $p < 0.05$ , t-test).

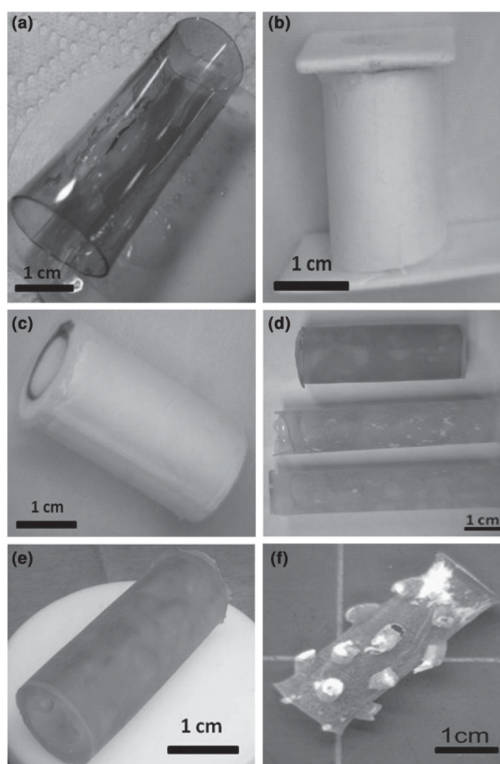


**Figure 7.**

Construction of biodegradable airway stents using APS. a) Reverse molding of APS showed high tension around seam. b,c) Porous Teflon molds for APS crosslinking. d,e) Airway stents of various sizes made of 1:2 APS.